SYSTEM ANALYSIS OF *PHYCOMYCES* LIGHT-GROWTH RESPONSE WITH SUM-OF-SINUSOIDS TEST STIMULI

PROMOD PRATAP, ANURADHA PALIT, AND EDWARD D. LIPSON
Department of Physics, Syracuse University, Syracuse, New York 13244-1130

ABSTRACT The light-growth response of *Phycomyces* has been studied with the sum-of-sinusoids method of nonlinear system identification (Victor, J. D., and R. M. Shapley, 1980, *Biophys. J.*, 29:459). This transient response of the sporangiophore has been treated as a black-box system with one input (logarithm of the light intensity, I) and one output (elongation rate). The light intensity was modulated so that $\log I$, as a function of time, was a sum of sinusoids. The log-mean intensity was 10^{-4} W m^{-2} and the wavelength was 477 nm. The first- and second-order frequency kernels, which represent the linear and nonlinear behavior of the system, were obtained from the Fourier transform of the response at the appropriate component and combination frequencies. Although the first-order kernel accounts for most of the response, there remains a significant nonlinearity beyond the logarithmic transducer presumed to occur at the input of the sensory transduction chain. From the analysis of the frequency kernels, we have derived a dynamic nonlinear model of the light-growth response system. The model consists of a nonlinear subsystem followed by a linear subsystem. The model parameters were estimated from a combined nonlinear least-squares fit to the first- and second-order frequency kernels.

INTRODUCTION

The sporangiophore of *Phycomyces blakesleeanus* modifies its growth in response to various stimuli including light, wind, barriers, pressure, gravity, and chemicals (Russo and Galland, 1980). The sporangiophore, which senses blue light over a range of 10^{10} in light intensity, shows two responses to light: it bends toward unilateral light (phototropism), and its elongation rate changes transiently in response to changes in light intensity (light-growth response; Foster and Lipson, 1973). The light-growth response is approximately linear with respect to the logarithm of light intensity (Foster and Lipson, 1973).

The light-growth response has been studied previously with system identification methods (Lipson, 1975*a*, *b*, *c*) involving "Gaussian white noise" stimuli (Marmarelis and Marmarelis, 1978). The Wiener kernels derived by this method represent the input-output relation of the system. These kernels are weighting functions that predict how the response of the system at a given time depends upon the recent history of the stimulus. Following the method of Victor and Shapley (1980), we have used a sum-of-sinusoids stimulus to derive the frequency kernels, which are essentially the Fourier transforms of the Wiener kernels of the system. Unlike the white-noise method, which employs a stochastic stimulus, the sum-of-sinusoids method uses a deterministic stimulus. Consequently, the kernels obtained by the sum-of-sinusoids method are more precise than those from the white-noise method (Victor, 1979).

Here, we first employ the system identification approach to obtain an "external" model that expresses the input-output relation of the light-growth response in terms of the frequency kernels. Then, using system analysis methods in the frequency domain, we consider several forms of "internal" parametric models to interpret mathematically the dynamic and nonlinear behavior of the system.

MATERIALS AND METHODS

Strains and Culture Conditions

The experiments were performed on the wild-type strain of *Phycomyces*, NRRL1555. Sporangiophores were grown in shell vials (12 mm diam × 35 mm high) filled to 10 mm from the top with potato dextrose agar medium (Difco Laboratories, Detroit, MI). An average of five spores were inoculated per vial. The vials were incubated in loosely closed glass jars under white fluorescent room light, until the first crop of sporangiophores was produced (~4 d after inoculation). The vials were then removed from the jars and placed in a growth chamber with overhead illumination provided by fluorescent lamps (Cool White, model F15T8-CW; GTE-Sylvania, Danvers, MA). The effective blue-light intensity in the chamber was 0.3 W m^{-2}, measured with a photodiode (model PIN-10DP; United Detector Technology, Santa Monica, CA), a broad-band blue filter (type 5-61; Corning Glass Works, Corning, NY) and a heat filter (model KG-1; Schott Optical Glass, Durea, PA). The sporangiophores were plucked each evening, so that a fresh crop would be available the next morning. Experiments were done on sporangiophores from the second and third crops only.

Phycomyces Tracking Machine

Experiments were performed on the *Phycomyces* tracking machine (Foster and Lipson, 1973; Lipson, 1975*a*). For each experiment, a

Address correspondence and reprint requests to Edward D. Lipson, Department of Physics, Syracuse University, Syracuse, NY 13244-1130.

sporangiophore in a vial was placed on the servo-controlled three-dimensional stage. To maintain the spherical sporangium (top of the sporangiophore) fixed in space, the stage moved continuously to compensate for the growth. The elongation rate of the sporangiophore was obtained directly from the vertical motion of the stage. To protect the sporangiophore from wind, the stage was housed inside a chamber, the temperature of which was maintained at 20°C.

Light Source

The stimulus light source was a 500-W tungsten-halogen lamp (model 500Q/CL; GTE-Sylvania). The light from the lamp passed through a heat filter and a 477-nm interference filter (Balzers B-40, 9–12-nm bandwidth, Rolyn Optics, Covina, CA) and then was focused by lenses onto the common end of a bifurcated fiber-optics light guide (Valtec, Inc., West Boylston, MA). The other two ends of the guide directed the light symmetrically and bilaterally onto the light-sensitive growing zone of the sporangiophore (which extends ~3 mm down from the sporangium) at an angle of ~30° below the horizontal. The light intensity at the growing zone was measured by a photodiode (model PIN-3DP; United Detector Technology) mounted on a holder that could be positioned by the stage of the tracking machine during calibration.

Control of Stimulus Light Intensity

The stimulus intensity was varied by a 4.0 OD circular neutral-density wedge (model A-6040; Eastman Kodak Co., Rochester, NY) placed between the lens system and the fiber-optics light guide. The wedge was rotated by means of a stepping motor (model M091-FC06; Superior Electric Company, Bristol, CT) and a 4:1 reduction gear (PIC Design Corp., Rockaway, NY). The wedge angle was controlled by a microcomputer (model Z-2; Cromemco Inc., Mountain View, CA) that calculated the sum-of-sinusoids signal and converted that to the wedge command voltage by means of a digital-to-analog converter board. The angular position of the wedge was fed back by means of a precision potentiometer mounted coaxially.

The Sum-of-Sinusoids Stimulus

The stimulus was a sum of 15 sinusoids. The frequencies of the individual sinusoidal components were multiples of a fundamental frequency, which was the inverse of the 273.1-min duration of the analyzed portion of the experiment (see below). The fundamental frequency was therefore 3.66×10^{-3} min^{-1}. The set of frequency multipliers used to calculate the sums of sinusoids was chosen so that the sums and differences of the frequencies (known as combination frequencies; note that the sum frequencies include the doubles of the component frequencies) were distinct from one another and from the component frequencies. An interactive program was written in UCSD Pascal (Softech Microsystems, San Diego, CA) to help choose such frequency sets without overlaps. The following set of 15 multipliers was used in the experiments: {7, 17, 33, 53, 71, 80, 92, 115, 147, 192, 249, 297, 338, 380, 473}. The stimulus was given at a log-mean intensity I_0 (defined by $\log I_0 = \langle \log I \rangle$, where the angle brackets represent a time average) of 10^{-4} W m^{-2} at a wavelength of 477 nm. The amplitude of each sinusoid was 0.2 decades.

Data Acquisition and Storage

At 8-s intervals, the computer recorded the stimulus (wedge angle from feedback potentiometer), the response (elongation rate of the sporangiophore), and the rectangular coordinates of the stage. Each experiment lasted 320 min.

Data Analysis

The first 46.9 min of the data were discarded; during this time, the sporangiophore was allowed to adapt to the stimulus conditions. Quadratic baselines were fit to both the stimulus and the response as a function of time, and then subtracted from them. This "detrending" (Marmarelis and Marmarelis, 1978) corrected for the slight acceleration of the sporangiophore growth. The stimulus and the response were then transformed to the frequency domain with a Fast Fourier Transform (FFT) algorithm (Stanley, 1975). The first- and second-order[1] frequency-domain kernels, H_1 and H_2, were calculated from the following relations (which follow from Eq. 19 of Victor and Shapley, 1980):

$$H_1(f) = \frac{R(f)}{S(f)}$$

$$H_2(f_1, f_2) = \frac{R(f_1 + f_2)}{S(f_1)\,S(f_2)}, \qquad (1)$$

where $S(f)$ and $R(f)$ are the Fourier transforms of the sum-of-sinusoids stimulus (actually of the wedge feedback voltage) and of the experimental response, evaluated only at the component and combination frequencies. The kernels for fifteen experiments were averaged. The zero-order kernel H_0, which is just the time average of the response, was zero because of the detrending (baseline removal).

The responses of several alternative internal models were fit to the experimental response at the component and combination frequencies. These fits were done on the campus computer (IBM 4341) with nonlinear least-squares algorithms (Marquardt, 1963; Hamilton, 1964) in the computer language APL. These algorithms provided standard errors for the parameter estimates and the normalized chi-square (goodness-of-fit parameter) of the fit. The normalized chi-square is the error-weighted sum of squares of residuals divided by the number of degrees of freedom; this is the quantity minimized by the least-squares procedure.

RESULTS

System Identification

Fig. 1 *a* shows a typical sum-of-sinusoids stimulus and Fig. 1 *b* the experimental response, averaged over 15 experiments. The frequency kernels (Figs. 2 and 3), which were extracted from the Fourier transform of the response, represent the input-output relation of the system. According to the sum-of-sinusoids method (Victor and Shapley, 1980), the response of a first-order external model to a sum-of-sinusoids stimulus

$$s(t) = \sum_{i=1}^{Q} a_i \cos\,(2\pi f_i t + \phi_i) \qquad (2)$$

[1] In this paper, we use the word order in two different senses, both of which are conventional. One is the order of nonlinearity. A strictly first-order system is one that is linear; if the stimulus to such a system has Fourier components at the frequencies $f_1, f_2, \ldots f_n$, the output will have Fourier components only at these frequencies. The response of a second-order (nonlinear) system to the same stimulus will have additional Fourier components at the frequencies $f_1 \pm f_2, f_1 \pm f_3, 2f_1, 2f_2$, and so on. In this sense, we speak of the first- and second-order kernels. The second usage of order is with reference to the dynamic order of a linear differential equation. A differential equation is of second order, for example, if the highest derivative present is d^2/dt^2. The transfer function for such a differential equation would have its highest-order frequency term f^2 (or, equivalently, s^2). In this dynamic sense, we refer to first- and second-order filters.

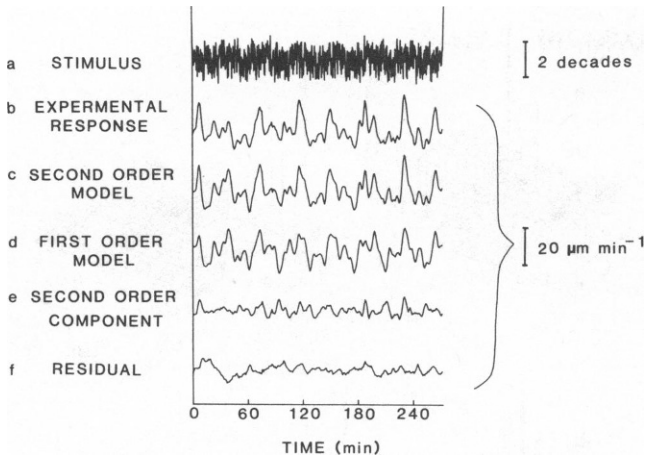

FIGURE 1 (*a*) Stimulus program consisting of a sum of 15 sinusoids, ranging in frequency from 0.026 min^{-1} (period: 39.0 min) to a maximum frequency of 1.732 min^{-1} (period: 0.577 min). The frequencies were chosen so that they were incommensurate (nonoverlapping) up to second-order combinations. The fundamental frequency was 0.0036 min^{-1}. The 15 frequency multipliers were 7, 17, 33, 53, 71, 80, 92, 115, 147, 192, 249, 297, 338, 380, and 473. All experiments were performed at a log-mean intensity $I_0 = 1 \times 10^{-4}$ W m^{-2} and at a wavelength of 477 nm. The temperature was 20.0 ± 0.5°C. (*b*) Experimental light-growth response (change in growth velocity) to stimulus in *a*. (*c*) Response to stimulus in *a* calculated (by substitution in Eq. 4 from first-order and second-order frequency kernels. (*d*) Response calculated from the first-order frequency kernel alone. (*e*) Contribution to the response from the second order kernel alone (*c* is the sum of *d* and *e*). (*f*) Residual between the experimental and model responses (difference between *b* and *c*).

is given by

$$r_1(t) = H_0 + 0.5 \sum_{i=-Q}^{Q} a_i H_1(f_i) \exp [j(2\pi f_i t + \phi_i)], \quad (3)$$

where H_0 and H_1 are the first- and second-order frequency kernels, and the subscript i refers to the ith sinusoid. In Eqs. 2 and 3, f_i is the component frequency and ϕ_i is the phase of the corresponding sinusoid, j is $(-1)^{1/2}$, and Q is the number of sinusoids in the sum-of-sinusoids stimulus.

The response of a second-order external model is given by

$$r_2(t) = r_1(t) + 0.25 \sum_{i=-Q}^{Q} \sum_{k=-Q}^{Q} \cdot a_i a_k H_2(f_i, f_k) \exp [j\{2\pi(f_i + f_k)t + \phi_i + \phi_k\}], \quad (4)$$

where H_2 is the second-order frequency kernel, r_1 is the expression in Eq. 3, and the subscripts i and k refer to the ith and the kth sinusoids.

To evaluate how well the experimental kernels $H_1(f)$ and $H_2(f_1, f_2)$ represent the system, we have substituted them into Eqs. 3 and 4, and thereby calculated the external model response to the experimental stimulus. This procedure is analogous to evaluating the results of a least-squares fit of data to a theoretical function, except that the procedure here is model independent (nonparametric). Fig. 1 *c* shows the response of the external model up to second order (r_2 in Eq. 4). The individual contributions from the first-order (given by Eq. 3) and second-order kernels (the second term on the right-hand side of Eq. 4) are shown in Figs. 1 *d* and 1 *e*, respectively. The residual between the experimental response and the predicted response is shown in Fig. 1 *f*.

Comparison of Figs. 1 *b* and 1 *d* shows that the first-order kernel alone describes the response quite well. The second-order kernel (Fig. 1 *e*) contributes much less than the first-order kernel. If the system were linear (i.e., obeying the principle of superposition), then the first-order kernel alone would suffice and the higher-order kernels would vanish. According to Fig. 1 *e*, though, the system has a small but significant nonlinearity beyond the logarithmic nonlinearity presumed to reside at the input. By applying the sum-of-sinusoids stimulus to the logarithm of the light intensity rather than to the intensity itself, we have effectively factored out the logarithmic transducer.

To quantify the improvement obtained by inclusion of the second-order kernel, we have calculated the mean-square difference between the experimental response and the external model responses computed from Eqs. 3 and 4 up to the zero-, first-, and second-order terms. Because of the detrending (baseline removal) procedure, the zero-order kernel is identically zero; therefore, the zero-order model response vanishes for all times. The mean-square error (MSE) between the experimental response and the zero-order model response (in other words, the variance of the detrended response) is 41.9 μm^2 min^{-2}. The MSE between the experimental response and the first-order model response is 30.4% of the response variance. Similarly, the MSE between the experimental response and the second-order model response is 15.5% of the response variance. Thus, inclusion of the second-order kernel in the external model reduces the MSE by half. The residual is

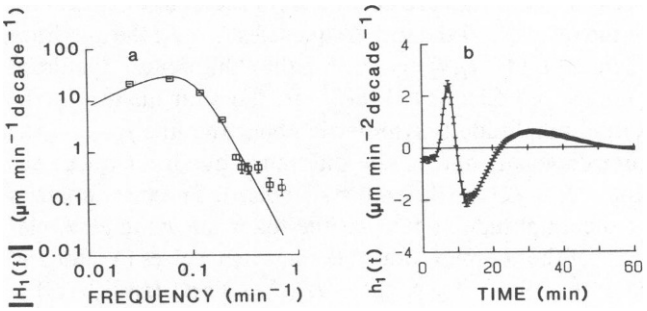

FIGURE 2 (*a*) Amplitude of first-order frequency-domain kernels obtained from response in Fig. 1 *b*. This amplitude includes only half of the information of the kernel; the phase is not shown. The experimental points are shown with error bars (standard errors for 15 experiments). The solid line is the first-order kernel of the internal model (Eq. 5). Fit of the model response at the component and combination frequencies to the experimental response gave the first- and second-order model kernels. (*b*) Average of the time-domain kernels of fifteen individual experiments obtained by Fourier transformation of the interpolated amplitude and phase.

attributable to contributions of higher-order kernels, and to experimental noise.

The first- and second-order frequency kernels were obtained directly (by means of Eq. 1) from the Fourier transforms of the stimulus (Fig. 1 *a*) and the detrended response (Fig. 1*b*). These kernels, which are calculated and analyzed in the frequency domain, are complex-valued functions. Fig. 2 *a* shows the amplitude of the first-order kernel as a function of frequency, plotted on double-logarithmic axes. The maximum of the first-order kernel occurs at a frequency $f_{max} = 0.06$ min^{-1}, beyond which the kernel falls off approximately as f^{-4}. The cutoff frequency f_c of the first-order kernel is defined conventionally as the frequency (beyond f_{max}) at which the kernel amplitude has fallen to 70.7% ($1/\sqrt{2}$) of the maximum value—in other words, the half-power level. For the kernel in Fig. 2 *a*, $f_c = 0.11$ min^{-1}. The values of f_{max} and f_c were determined from the maximum in the model kernel (solid line in Fig. 2 *a*).

The first-order time-domain kernel of the system is shown in Fig. 2 *b*. We obtained this time-domain kernel by interpolating and Fourier transforming the amplitude (Fig. 2 *a*) and phase (not shown) of the frequency-domain kernel. The interpolation is necessary because the Fast Fourier Transform algorithm requires the kernel at uniformly spaced frequencies (the sum-of-sinusoids component frequencies are necessarily nonuniformly spaced). This kernel shows the usual latency of ~4 min for the light-growth response (Foster and Lipson, 1973; Lipson, 1975*b*), as well as a maximum at ~7.5 min and a minimum at 13 min.

Fig. 3 *a* shows the amplitude of the second-order frequency kernel $H_2(f_1, f_2)$, which is obtained from the Fourier transform of the response (Fig. 1 *b*) at the combination frequencies (sums and differences of the sum-of-sinusoids component frequencies). The quadrant on the right with axes (f_1, f_2) is termed the "sum" quadrant, because the values are derived from the Fourier transform of the response at the sum frequencies $f_1 + f_2$; the quadrant spanned by $(-f_1, f_2)$ is termed the "difference" quadrant (Victor and Shapley, 1980)[2]. In the sum quadrant, the kernel amplitude is symmetric about the line $f_1 = f_2$ (the sum diagonal) and in the difference quadrant about the line $-f_1 = f_2$ (the difference diagonal). These symmetries of the amplitude arise from the following symmetry relations of the complex-valued kernels themselves (Victor and Shapley, 1980): $H_2(f_1, f_2) = H_2(f_2, f_1)$ and $H_2(f_1, -f_2) = H_2^*(f_2, -f_1)$, where H_2^* is the complex conjugate of H_2. Along the difference diagonal, the combination frequencies $(f_i - f_i$, where i is an index for the component frequencies of the sum-of-sinusoids stimulus) are all zero, so that these combinations all contribute to the zero-frequency (DC) value of the response and cannot be resolved (Victor and Shapley, 1980). For this reason, the values of H_2 are inaccessible along the difference diagonal.

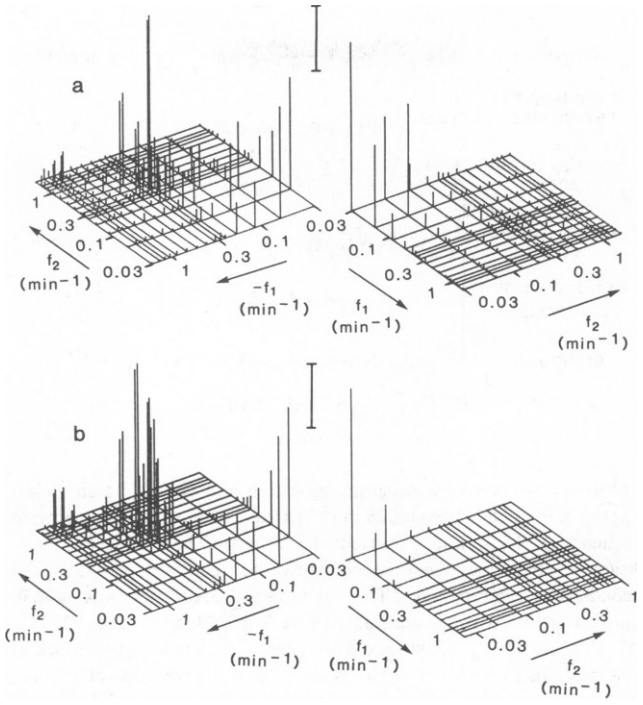

FIGURE 3 (*a*) Second-order frequency kernel for the same set of experiments as in Figs. 1 and 2. The ordinate is the amplitude of the complex-valued kernel, $H_2(f_1, f_2)$. The frequency abscissae are logarithmic. The amplitude of $H_2(f_1, f_2)$ is plotted on the right (sum quadrant), and the amplitude of $H_2(-f_1, f_2)$ is plotted on the left (difference quadrant). (*b*) Second-order kernel of the internal model represented by Eq. 5, obtained from the fits of the experimental response to the model response at the component and combination frequencies. The scale bar represents 20 μm min^{-1} decade^{-2}.

In the difference quadrant, the kernel shows two peaks: one at the low-frequency pair (0.026, 0.062 min^{-1}) and another at the intermediate-frequency pair (0.29, 0.34 min^{-1}). Both peaks lie close to the difference diagonal; in this region, the difference frequencies are smaller than the cutoff frequency ($f_c = 0.11$ min^{-1}) of the first-order kernel. The kernel becomes negligible at points away from this diagonal, because the difference frequencies extend beyond the system bandwidth, so they cannot appear significantly in the experimental response. For the intermediate-frequency peak, the component frequencies (i.e, those in the sum-of-sinusoids stimulus) are both well above the cutoff frequency of the first-order kernel. Although the system will not respond to individual sinusoids at these frequencies, it can respond (at the difference frequency, if sufficiently small) to a sum of two such sinusoids.

The response at the combination frequencies is due to the nonlinearity in the system. For the response at a particular combination frequency to be large, the nonlinear subsystem that contributes at this combination frequency must receive substantial signal amplitudes (i.e. Fourier

[2]Note: the usage of f_1 and f_2 here for the two axes of the second-order frequency kernels should not be confused with the component frequencies f_i with $i = 1, \ldots, 15$.

component amplitudes) at the corresponding component frequencies. In other words, these component frequencies must not be highly attenuated by dynamic filters before their arrival at the nonlinear subsystem. Because the system can respond to difference combinations of high frequencies (each larger than the overall bandwidth), the nonlinearity must occur towards the input of the system, before the element that determines the system bandwidth.

The ratio of the root-mean-square value of the second-order kernel to that of the first-order kernel has been used as a numerical measure of the strength of the nonlinearity. For the experiments shown here, we obtained a value of 0.58 decade^{-2} for the strength of nonlinearity. This will serve as a basis of comparison in the following two papers.

System Analysis

The external model of the system, represented by the experimental kernels, can be interpreted by standard methods of system analysis. Such methods are normally applied in the frequency domain, for reasons of convenience and simplicity (namely, convolution integrals in the time domain transform to simple algebraic products in the frequency domain, according to the convolution theorem of Fourier analysis).

To interpret the experimental results, we have developed several dynamic models based on the structure of the experimental kernels. Such internal models, each with several adjustable parameters, can be fit to the external model (i.e. the experimental kernels) by nonlinear least-squares techniques. To construct internal models, we have adopted a building-block approach. The components that serve as the building blocks are linear filters[3] of first and second order, and static (i.e., instantaneous or memoryless) nonlinear elements. A similar approach was taken by Victor and Shapley (1979, 1980).

It is common in the frequency-domain analysis of dynamic systems to employ the theory of Laplace transforms as an alternative to Fourier analysis. In this approach, the frequency f is supplanted by the Laplace transform variable s. For the present purposes, s can be related simply to f by the equation $s = j2\pi f$. Thus s is directly proportional to the frequency.

We have considered several models for a dynamic nonlinear system based on the general form shown in Fig. 4 a. The boxes P, Q, R, and W in Fig. 4 *a* each represent dynamic linear elements (filters), while the box S is a static squarer. The first-order kernel of this model system is $R(s)W(s)$ and the second-order kernel is $W(s_1 + s_2)Q(s_1 + s_2)P(s_1)P(s_2)$ (Victor and Shapley, 1979), where P, Q, R, and W are the first-order frequency

[3]A filter is a dynamic system, and is classified in terms of its frequency response: a high-pass filter responds preferentially to high-frequency stimuli, while a low-pass filter responds more to low-frequency stimuli. A linear filter can be represented mathematically in terms of its transfer function.

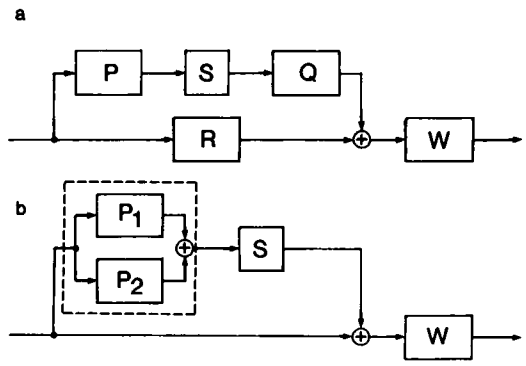

FIGURE 4 (*a*) A generalized model with a dynamic second-order nonlinear subsystem toward the input. The boxes P, Q, R, and W are dynamic linear systems. The box S is a squarer. The first-order (linear) response is due just to the boxes R and W. The second-order (nonlinear) response is due to squarer S. The boxes P and Q make the nonlinear path itself dynamic. (*b*) The model that provides the best fit to the data. This is a special case of the model in *a*, with boxes Q and R replaced with identity operators. Box P has been split into two parallel boxes P_1 and P_2. Box P_1 is a second-order low-pass filter and box P_2 is a high-pass filter. Box W is a fifth-order linear system described by the analytical transfer function (Eq. 5d) proposed by Lipson (1975*a*).

kernels of the filters. If $P = 1$ and Q and R are (static) amplifiers, then the output of the summing element reduces to a quadratic polynomial ($z = rx + qx^2$), where r and q are constant coefficients. Thus the entire subsystem to the left of W is a generalization of a static nonlinearity to include dynamics.

We have fit the data to models with various choices for P, Q, R, and W. For each model, we estimated the parameters from fits of the model response to the experimental response. The normalized chi-square (the error-weighted sum of squares of residuals divided by the number of degrees of freedom) served as a goodness-of-fit parameter. The best internal model (Fig. 4 *b*) gave the minimum normalized chi-square. In this model, the box P is decomposed in the sum of two subsystems P_1 and P_2 so that the transfer function of P is $P(f) = P_1(f) + P_2(f)$. For this model, the frequency kernels have the following analytical forms

$$P(s) = \frac{\beta_{N1}}{s^2 + (2\alpha_{N1})(2\pi f_{N1})s + (2\pi f_{N1})^2} + \frac{\beta_{N2}s}{[s^2 + (2\alpha_{N2})(2\pi f_{N2})s + (2\pi f_{N2})^2]^n} \quad (5a)$$

$$Q(s) = 1 \quad (5b)$$

$$R(s) = 1 \quad (5c)$$

$$W(s) = \beta_L e^{-st_0}\left[\frac{s}{s + 2\pi f_{L1}}\right] \cdot \left[\frac{(2\pi f_{L2})2}{s^2 + (2\alpha_L)(2\pi f_{L2})s + (2\pi f_{L2})^2}\right]^2, \quad (5d)$$

where the subscripts N and L identify those parameters

associated with the nonlinear subsystem (the part of Fig. 4 *a* to the left of the summing element, inclusive of the boxes *P*, *S*, *Q*, and *R*) and the linear subsystem (*W*), respectively. The form for $W(s)$ is identical to the analytical transfer function of Lipson (1975*a*), rewritten with the new subscript L. The first- and second-order kernels of this internal model are shown in Fig. 2 *a* (solid line) and Fig. 3 *b*.

The parameters of the linear transfer function *W* (which represents the first-order frequency kernel $H_1(f)$) are

$$\beta_L = 49 \pm 22\ \mu\text{m min}^{-1}\ \text{decade}^{-1}$$
$$f_{L1} = 0.063 \pm 0.033\ \text{min}^{-1}$$
$$f_{L2} = 0.106 \pm 0.009\ \text{min}^{-1}$$
$$\alpha_L = 0.75 \pm 0.07$$
$$t_0 = 3.93 \pm 0.08\ \text{min},$$

where β_L is an overall gain factor, f_{L1} is the cutoff frequency of the first-order filter, f_{L2} and α_L are the cufoff frequency and damping constant, respectively, of the two identical second-order filters, and t_0 is the latency.

The estimated parameters for the elements of the nonlinear subsystem are

$$\beta_{N1} = 0.125 \pm 0.003\ \text{decade}^{-1/2}\ \text{min}^{-2}$$
$$f_{N1} = 0.032 \pm 0.002\ \text{min}^{-1}$$
$$\alpha_{N1} = 1.22 \pm 0.34$$
$$\beta_{N2} = 0.63 \pm 0.09\ \text{decade}^{-1/2}\ \text{min}^{-2n+1}$$
$$f_{N2} = 0.35 \pm 0.02\ \text{min}^{-1}$$
$$\alpha_{N2} = 0.183 \pm 0.072$$
$$n = 0.41 \pm 0.05,$$

where β_{N1}, f_{N1}, and α_{N1} are the gain factor, the cutoff frequency, and the damping constant of the second-order low-pass filter P_1, and β_{N2}, f_{N2}, and α_{N2} are those for the high-pass filter P_2 (Fig. 4 *b*). The parameter *n* is an exponent in the high-pass filter P_2.

DISCUSSION

We have treated the *Phycomyces* light-growth response system as a black box, with one input, the logarithm of the light intensity, and one output, the change in the elongation rate. Our work has proceeded in two steps: the first step, system identification, involved the determination of the frequency kernels (Fourier transforms of the Wiener kernels of the system) with the sum-of-sinusoids method. The second step, system analysis, involves the interpretation of these kernels, which reflect the dynamic properties of the system. To interpret the kernels, we have developed and tested models with guidance from the structure of the kernels.

Dynamic Nature of the Nonlinearity

Because the light-growth response is approximately linear with the logarithm of the light intensity, a logarithmic transducer is presumed to occur at the input of the system (Bergman et al., 1973; Lipson, 1975*a*). We have, in effect, factored this static nonlinearity out of the system by using $\log I$ as the input instead of the intensity I. Further, the use of $\log I$ permits the system to be tested over a much greater range, so that any additional nonlinear behavior can be exposed (Lipson, 1975*b*). Because the presumed nonlinearity at the beginning of the transduction chain may not be strictly logarithmic, the observed nonlinear behavior (from the experimental second-order kernel) could conceivably be just a correction to the hypothetical logarithmic transducer. However, the intrinsically dynamic nature of the nonlinearity, as discerned from the structure of the second-order kernel, indicates that it cannot be simply a static correction.

Internal Model Parameters

The linear subsystem *W* (Fig. 4; Eq. 5d) contains the following elements: an overall gain factor (β_L), a delay term (to account for the latency t_0 of the light-growth response), a first-order high-pass filter, and two identical second-order low-pass filters. The first-order high-pass filter has been previously considered in the framework of adaptation (Lipson, 1975*a*). The nonlinear subsystem (Fig. 4) contains a squarer preceded by a second-order low-pass filter in parallel with a high-pass filter (Eq. 5a).

The two identical second-order filters in the first-order model kernel are underdamped ($\alpha < 1$). Such filters can represent biochemical reactions with feedback (P. Pratap, Ph.D. dissertation). For the second-order kernel, the damping constant α_{N1} of the second-order low-pass filter is unity (critical damping), within errors. In the case of critical damping, the second-order low-pass filter (box P_1 in Fig. 4 *b*) can be factored into two identical first-order low-pass filters in cascade. Each first-order filter could then represent a monomolecular reaction (Capellos and Bielski, 1972).

Advantages of the Sum-of-Sinusoids Method

In comparison to the white-noise method of nonlinear system identification (Marmarelis and Marmarelis, 1978), the sum-of-sinusoids method offers several advantages (Victor and Shapley, 1980). It is numerically easier to apply, both in the calculation of the kernels and in tests of models. The calculation of kernels involves simple algebraic manipulation (Eq. 1) of the Fourier transforms of the experimental response and the stimulus. We have compared the errors of the first-order frequency kernels presented in this paper with the errors of kernels calculated by the white-noise method (Poe and Lipson, 1986). In this

comparison, the sum-of-sinusoids method is about four times more precise than the white-noise method.

In our experience, a considerable advantage of the sum-of-sinusoids method is that it provides an efficient way for both the linear and nonlinear kernels to be fit jointly to any model. In contrast, in the white-noise method, this type of fitting is very difficult to accomplish, because the only way to put the linear and nonlinear kernels on the same basis (dimensionally and otherwise) is to compute the Wiener series itself for each experimental time point. Specifically, to perform an iterative nonlinear least-squares fit of an internal model to a set of experimentally derived kernels (in both the sum-of-sinusoids and the white-noise methods), one must generate the external model response at each iteration. In the white-noise method, prodigious amounts of computer time are required for the evaluation of the convolution integrals, especially those of second order. In the sum-of-sinusoids method, the procedure is remarkably simple, because the frequency kernels are obtained directly from the Fourier transform of the experimental response. Except for known scale factors, the frequency kernels are just the values of this transform at the component frequencies (first-order kernel), or at the sum and difference frequencies plus the doubles of the component frequencies (second-order kernel). Therefore, in the frequency domain, the convolution integrals reduce to algebraic relations, and the model response can be computed simply and rapidly at each iteration.

Conclusions

From the experimental first- and second-order kernels, we have developed a dynamic, nonlinear model of the light-growth response. The residual nonlinearity (beyond the presumed logarithmic transducer) lies toward the input of the system. Specifically, the best model—according to our fitting procedures—places the dynamic nonlinearity near the input of the system, before the linear subsystem W.

There is degeneracy in the model in that the filters in the linear subsystem can be arranged in any order, because linear systems are commutative. On the basis of a model for dark adaptation, Lipson (1975*a*) had speculated on the order of the elements of the linear subsystem; specifically, the latency and the second-order low-pass filters in the linear subsystem may occur toward the output of the sensory transduction pathway.

Recent evidence indicates that dark adaptation is wavelength dependent (Galland et al., 1984) and that certain behavioral mutants are affected in the photoreceptor system (Galland and Lipson, 1985). In the two subsequent papers, we will analyze the light-growth response system at different wavelengths, temperatures, and with mutants.

We are grateful to Robert Shapley and Jonathan Victor for helpful advice on the application of the sum-of-sinusoids method. We thank Randall Poe for his participation in the early parts of this work, in particular for software development, and Dave Durant for his help in interfacing the microcomputer to the tracking machine. Finally, we are indebted to Paul Galland and Benjamin Horwitz for valuable discussions and for comments on the manuscript.

This work was supported by grant GM29707 from the National Institutes of Health to Edward D. Lipson.

Received for publication 24 January 1986.

REFERENCES

Bergman, K., A. P. Eslava, and E. Cerda-Olmedo. 1973. Mutants of *Phycomyces* with abnormal phototropism. *Mol. Gen. Genet.* 123:1–16.

Capellos, C., and B. H. J. Bielski. 1972. Kinetic Systems. Mathematical Description of Chemical Kinetics in Solution. Wiley-Interscience, New York. 49–51.

Foster, K. W., and E. D. Lipson. 1973. The light growth response of *Phycomyces*. *J. Gen. Physiol.* 62:590–617.

Galland, P., and E. D. Lipson. 1985. Modified action spectra of photogeotropic equilibrium in *Phycomyces blakesleeanus* mutants with defects in genes *madA, madB, madC,* and *madH*. *Photochem. Photobiol.* 41:331–335.

Galland, P., A. S. Pandya, and E. D. Lipson. 1984. Wavelength dependence of dark adaptation in *Phycomyces* phototropism. *J. Gen. Physiol.* 84:739–751.

Hamilton, W. C. 1964. Statistics in Physical Science. Estimation, Hypothesis Testing, and Least Squares. Ronald Press Co., New York.

Lipson, E. D. 1975*a*. White noise analysis of *Phycomyces* light growth response system. I. Normal intensity range. *Biophys. J.* 15:989–1012.

Lipson, E. D. 1975*b*. White noise analysis of *Phycomyces* light growth response system. II. Extended intensity ranges. *Biophys. J.* 15:1013–1032.

Lipson, E. D. 1975*c*. White noise analysis of *Phycomyces* light growth response system. III. Photomutants. *Biophys. J.* 15:1033–1045.

Marmarelis, P. Z., and V. Z. Marmarelis. 1978. Analysis of Physiological Systems. The White Noise Approach. Plenum Press, New York.

Marquardt, D. W. 1963. An algorithm for least-squares estimation of nonlinear parameters. *J. Soc. Indust. Appl. Math.* 11:431–441.

Poe, R. C., and E. D. Lipson. 1986. System analysis of *Phycomyces* light-growth response with Gaussian white noise test stimuli. *Biol. Cybern.* In press.

Russo, V. E. A., and P. Galland. 1980. Sensory physiology of *Phycomyces blakesleeanus*. *Struct. Bonding.* 47:71–110.

Stanley, W. D. 1975. Digital Signal Processing. Reston Publishing Co., Reston, VA. 256–273.

Victor, J. D. 1979. Nonlinear systems analysis: comparison of white noise and sum of sinusoids in a biological system. *Proc. Natl. Acad. Sci. USA.* 76:996–998.

Victor, J. D., and R. M. Shapley. 1979. Nonlinear pathways of the Y ganglion cells in the cat retina. *J. Gen. Physiol.* 74:671–689.

Victor, J. D., and R. M. Shapley. 1980. A method of nonlinear analysis in the frequency domain. *Biophys. J.* 29:459–484.